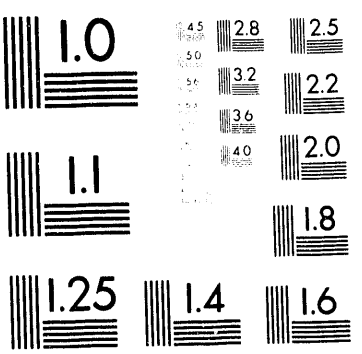
1.0
1.1
1.25
1.4
1.6
1.8
2.0
2.2
2.5
2.8
3.2
3.6
4.0
4.5
5.0

1 of 1

MEASURING LIQUID PROPERTIES WITH SMOOTH- AND TEXTURED-SURFACE RESONATORS

S. J. Martin, K. O. Wessendorf, C. T. Gebert, G. C. Frye,
R. W. Cernosek, L. Casaus, and M. A. Mitchell

Sandia National Laboratories, Albuquerque, New Mexico

Abstract

The response of thickness shear mode (TSM) resonators in liquids is examined. Smooth-surface devices, which viscously entrain a layer of contacting liquid, respond to the product of liquid density and viscosity. Textured-surface devices, which also trap liquid in surface features, exhibit an additional response that depends on liquid density alone. Combining smooth and textured resonators in a monolithic sensor allows simultaneous measurement of liquid density and viscosity.

Introduction

The sensitivity of quartz resonators to surface mass accumulation enables their use in a number of sensing applications. The linear change in resonant frequency that occurs with mass accumulation allows the device to function as a general-purpose gravimetric detector or "microbalance." The device is easily instrumented as a sensor by incorporating it as the frequency-control element of an oscillator circuit. Resonators were initially used as thickness monitors in vacuum deposition systems [1]. Later, chemically-sensitive films were added to form gas and vapor detectors [2].

Certain resonator modes permit liquid sensor operation also [3]. Compressional modes couple too strongly to the contacting liquid, generating sound waves that "leak away" acoustic energy and suppress resonance. Shear-modes, however, couple less strongly to the liquid and

resonant characteristics are preserved. Thus, TSM resonators can be successfully operated in liquids, provided a specially-designed oscillator circuit is used that overcomes the substantial liquid damping [4]. Device mass sensitivity is preserved in liquids, permitting a number of liquid-phase sensing applications to be addressed [5-7].

TSM resonators can also be used to probe liquid properties. For example, Kanazawa and Gordon have shown that the mechanical interaction between TSM resonators and a contacting liquid results in a change in resonant frequency that depends on liquid density and viscosity [8]. In this paper, we consider how such interactions can be used to probe liquid properties and the role of surface texture in extending this capability.

Smooth-Surface Devices

Fig. 1 shows the cross-sectional displacement profile for the fundamental TSM in an AT-cut quartz resonator. This mode is electrically excited by applying an RF bias to electrodes at the upper and lower crystal surfaces. A thin mass layer that is rigidly bound to the surface moves synchronously with the oscillating surface. When a smooth device is operated in contact with a liquid, the oscillating surface generates plane-parallel laminar flow in the adjacent liquid, as shown in Fig. 1. This "viscously coupled" liquid undergoes a phase lag that increases with distance from the surface.

Fig. 2 shows an equivalent circuit model that describes the near-resonant electrical characteristics of the mass- and/or liquid-loaded TSM resonator [9]. The left branch of the circuit accounts for the "static" capacitance, C_o, that arises between electrodes across the insulating quartz plus parasitic capacitance, C_p, in the test fixture: $C_o^* = C_o + C_p$. The right branch accounts for the "motional impedance" that arises from charges induced on the electrodes

by the electrically-excited shear mode resonance. The elements L_1, C_1, and R_1 describe the motional impedance of the unperturbed (without mass or liquid loading) resonator.

Liquid contact causes an increase in the motional impedance that is accounted for by the motional inductance L_2 and resistance R_2. These can be related to the unperturbed motional impedance L_1 and properties of a contacting Newtonian liquid by [9]:

$$L_2 = \frac{nL_1}{N\pi}\left(\frac{2\omega_s\rho\eta}{\rho_q\mu_q}\right)^{\frac{1}{2}} \tag{1a}$$

$$R_2 = \frac{n\omega_s L_1}{N\pi}\left(\frac{2\omega_s\rho\eta}{\rho_q\mu_q}\right)^{\frac{1}{2}} \tag{1b}$$

where ω_s is the angular series resonant frequency, i.e., where $\omega_s=1/((L_1+L_2+L_3)C_1)^{1/2}$, n is the number of immersed resonator faces, N is the harmonic number of the TSM, ρ and η are liquid density and viscosity, while ρ_q and μ_q are the quartz density and shear stiffness. (In addition to changing the motional impedance, the liquid dielectric typically affects the parasitic capacitance C_p also.) The motional inductance L_2 represents kinetic energy stored in liquid moving synchronously with the device surface while R_2 represents viscous power dissipation. Energy storage and power dissipation are proportional for Newtonian liquids: $R_2 = \omega_s L_2$.

A surface mass layer that is thin and rigid so that displacement is uniform across the film causes only an increase in motional inductance given by [9]:

$$L_3 = \frac{2n\omega_s L_1\rho_s}{N\pi\sqrt{\rho_q\mu_q}} \tag{2}$$

where n is the number of coated sides and ρ_s is the areal mass density (mass/area) on each side:

$\rho_s = \rho h$, where ρ is the density and h is the thickness of the layer. L_3 represents the kinetic energy of the mass layer moving synchronously with the oscillating crystal surface. Since the film is assumed to be rigid and thus unstrained, no power is dissipated in this process and no motional resistance contribution arises.

The effect of a mass layer or liquid contact on the electrical response of a TSM resonator can be predicted from the equivalent circuit model of Fig. 2. The parameters relating to the unperturbed device (L_1, C_1, R_1, and C_0^*) are determined by fitting the model (with L_2, R_2, and L_3 set to zero) to electrical measurements made on the unperturbed device. Then the response arising from mass- or liquid-loading is determined from the model using element values for L_2, R_2, and L_3 calculated from Eqs. 1 and 2 on the basis of the mass density (ρ_s) or the product of liquid density and viscosity ($\rho\eta$).

Fig. 3 shows electrical admittance-*vs.*-frequency measurements (points) made on a liquid-contacted TSM resonator as solution properties were changed. Several glycerol/water mixtures of varying density ρ and viscosity η contacted the device on one side (n=1). As $\rho\eta$ increases, the resonant frequency decreases, while the resonance becomes increasingly damped. The solid lines in Fig. 3 are calculated from the equivalent circuit model with L_2 and R_2 determined from Eqs. 1 using literature values of liquid density and viscosity. The results show that the motional elements described by Eqs. 1 adequately describe the changes in motional impedance caused by liquid contact.

Fig. 4 illustrates the effect of a mass layer on the TSM resonator response. Admittance-vs.-frequency measurements are shown for a resonator before and after addition of a 124 nm gold layer to one side. Responses were measured for the device in air and contacted on the

same side by water. The major effect of the gold layer is to *translate* the admittance curves toward a lower resonant frequency without affecting the admittance magnitude or phase angle. The solid lines in Fig. 4 are admittances calculated from the equivalent circuit model using a best-fit inductance L_3=188 μH. From Eq. 2, this L_3 value corresponds to a surface mass density ρ_s=225 μg/cm^2, indicating a gold thickness (ρ=19.3 g/cm^3 for bulk gold) of 117 nm--within 6% of the thickness determined from profilometry measurements (124 nm). Thus, the motional inductance given by Eq. 2 adequately describes the change in motional impedance contributed by a surface mass layer. Moreover, the equivalent circuit model describes the electrical response for *combined* mass and liquid loading (Fig. 4, curve D).

Changes in the series resonant frequency, Δf_s, and the total motional resistance, ΔR_m, due to mass and/or liquid loading can be determined from the equivalent circuit model of Fig. 2 [9]:

$$\Delta f_s \cong -\frac{(L_2 + L_3) f_s}{2L_1} = -\frac{2nf_s^2}{N\sqrt{\rho_q \mu_q}}\left[\rho_s + \left(\frac{\rho\eta}{4\pi f_s}\right)^{\frac{1}{2}}\right] \tag{3a}$$

$$\Delta R_m = R_2 = \frac{n\omega_s L_1}{N\pi}\left(\frac{2\omega_s \rho \eta}{\rho_q \mu_q}\right)^{\frac{1}{2}} . \tag{3b}$$

Eq. 3a indicates that both mass and liquid loading act to decrease the resonant frequency of a TSM resonator. Consequently, measurement of the resonant frequency alone is insufficient to discriminate changes in surface mass from changes in contacting fluid properties. However, if the motional resistance (R_m) is also measured, then $\rho\eta$ is determined from Eq. 3b; this allows the fluid contribution to Δf_s to be determined (second term of Eq. 3a); the remaining frequency shift can be attributed to ρ_s. Thus, mass loading can be quantified simultaneously with fluid

properties ($\rho\eta$) if both resonant frequency changes (Δf_s) and crystal damping (R_m) are measured.

With regard to discriminating liquid properties, we note that these enter into the model above only as a product of liquid density and viscosity ($\rho\eta$). This indicates that *a smooth-surfaced TSM resonator is incapable of resolving liquid density and viscosity*. This shortcoming is remedied by including a device with surface texture.

Textured-Surface Devices

Devices with surface texture, either randomly rough or regularly patterned, trap a quantity of liquid in excess of that entrained by a smooth surface [5,10,11]. Vertical features constrain this trapped liquid to move synchronously with the oscillating crystal surface, rather than undergoing a progressive phase lag as occurs with viscously coupled liquid. This trapped liquid thus *behaves as an ideal mass layer* contributing an areal mass density $\rho_s = \rho h$, where ρ is the density and h is now the effective thickness of the trapped liquid layer--dependent upon the vertical relief of the surface texture. If this trapped liquid thickness is small compared to the liquid decay length $\delta = (2\eta/\omega\rho)^{1/2}$ [8], then the surface is considered hydrodynamically smooth and the relative response due to liquid trapping is negligible. If h is comparable or larger than δ, however, then a significant *additional frequency shift arises* from trapping in the textured surface that is dependent only on density and not on viscosity. Thus, a pair of devices, one smooth and one with a textured surface, allows liquid density and viscosity to be resolved.

From Eq. 3a, the frequency shifts that occur upon immersion of a smooth- (Δf_1) and a textured-surface (Δf_2) device can be written as:

where c_1, c_1', and c_2 are constants. If the surface texture is not too large, the contribution to

$$\Delta f_1 = -c_1\sqrt{\rho\eta} \tag{4a}$$

$$\Delta f_2 = -c_1'\sqrt{\rho\eta} - c_2 h\rho \tag{4b}$$

viscous entrainment of liquid is nearly unchanged from the smooth-surface case, i.e., $c_1' \cong c_1$.

From Eqs. 4, the liquid density can be obtained from the difference in responses measured between the smooth and textured devices upon immersion:

$$\rho = \frac{\Delta f_1 - \Delta f_2}{c_2 h} \quad . \tag{5}$$

assuming $c_1' = c_1$.

Having determined liquid density, the response of the smooth device can then be used (Eq. 4a) to determine liquid viscosity:

$$\eta = \frac{(\Delta f_1)^2}{c_1^2\rho} = \frac{c_2 h(\Delta f_1)^2}{c_1^2(\Delta f_1 - \Delta f_2)} \quad . \tag{6}$$

Alternatively, if the motional resistance R_m is measured, liquid viscosity can be determined from this parameter: Eq. 3b indicates that for a smooth device, $\Delta R_m = c_3(\rho\eta)^{1/2}$, from which

$$\eta = \frac{1}{\rho}\left(\frac{\Delta R_m}{c_3}\right)^2 \quad . \tag{7}$$

Dual-Resonator Sensor for Density and Viscosity Measurement

Fig. 5 shows a monolithic quartz sensor that includes smooth and textured TSM resonators to measure liquid density and viscosity. Since these liquid properties (especially

viscosity) are temperature dependent, a meander-line resistance temperature device (RTD) is included for measuring liquid temperature. Texture in the form of a surface corrugation is formed on one device by electrodepositing periodic gold ridges on top of the gold electrodes. In order to trap liquid and insure that it moves synchronously with the surface, these ridges are oriented perpendicular to the direction of surface shear displacement--the +X crystalline direction.

In fabricating the dual-resonator device, a Cr/Au (30 nm/200 nm) metallization layer is first deposited on both sides of an optically polished AT-cut quartz wafer. This metallization layer is photolithographically patterned to form the resonator electrodes (both sides) and the meander-line RTD (one side). A periodic resist pattern is formed on both electrodes of the resonator whose surface is to be textured. Gold is electrodeposited in the exposed electrode regions to a thickness of 1.5 μm. When the photoresist is removed, a corrugation pattern remains (Fig. 6) with trapezoidal cavities approximately 4.6 μm wide at the base that are well suited for trapping liquid.

The dual-resonator sensor is instrumented for liquid density and viscosity determination as shown in Fig. 7. Each resonator is driven by an independent oscillator circuit that provides two outputs [4]: an RF signal that tracks f_s and a DC voltage proportional to R_m. The RF outputs from the oscillators are read by frequency counters while the DC voltages and RTD resistance are read by multimeters. These signals are input to a personal computer. The baseline responses are determined by measuring f_s and R_m for each device before immersion. Changes in responses are then measured for the smooth (Δf_1, ΔR_1) and corrugated (Δf_2, ΔR_2) devices after immersion; liquid properties are then determined from Eqs. 5 - 7.

Fig. 8 illustrates the *densitometer function* of the dual-resonator sensor of Fig. 5. The difference in responses ($\Delta f_1 - \Delta f_2$) measured between the smooth and corrugated resonators upon immersion (2 sided liquid contact) is shown vs. liquid density. The response difference is extremely linear with density, following Eq. 5, despite variations in viscosity between the test liquids.

Fig. 9 illustrates the *viscometer function* of the dual-resonator sensor. The variations in oscillation frequency and motional resistance for the smooth and corrugated resonators are shown vs. the liquid parameter $(\rho\eta)^{1/2}$. In the upper plot, the network analyzer data (dashed line) indicate that f_s varies linearly with $(\rho\eta)^{1/2}$, as expected from Eq. 3a. The oscillator follows f_s at low values of damping, but deviates as damping increases, introducing a non-linear response in Δf vs. $(\rho\eta)^{1/2}$. The lower plot indicates that the oscillators are capable of driving the resonators for R_m values up to approximately 3.5 KΩ. R_m increases more linearly with the damping parameter $(\rho\eta)^{1/2}$ and is thus a good alternative to using Δf_s for extracting liquid viscosity.

Fig. 10 shows a "scatter diagram" that compares liquid densities and viscosities extracted from dual-resonator measurements (circles) with literature values (squares). The liquid corresponding to each set of points is indicated in Table I. With 2-sided liquid contact, the crystal becomes damped too severely to sustain oscillation for $\rho\eta > 8$. Since liquid damping increases (Eq. 1b) as $n(\rho\eta)^{1/2}$, limiting liquid contact to a single side extends the $\rho\eta$ range to 32. This data illustrates that liquid density and viscosity can be extracted from measurements made by a pair of quartz resonators--one smooth and one textured. The average differences between the measured and literature values were 5.3% for density and 19.5% for viscosity.

Conclusion

Quartz resonators with smooth surfaces can be operated in liquids to measure surface mass accumulation and the density-viscosity product of a contacting fluid. By measuring both Δf_s and ΔR_m, surface mass can be differentiated from the fluid parameter $\rho\eta$. Surface texture on the resonator traps fluid, which behaves as a mass layer, contributing an additional response proportional to liquid density. Comparing the responses of a pair of resonators--one smooth and one textured--enables liquid density to be extracted. Once density is known, the response of a smooth device yields liquid viscosity.

Acknowledgements

The authors wish to thank Prof. S. D. Senturia of the Massachusetts Institute of Technology for helpful discussions and K. Rice of Sandia National Laboratories for graphical assistance. This work was performed at Sandia National Laboratories, supported by the U.S. Department of Energy under contract No. DE-AC04-76DP00789.

References

[1] Sauerbrey, G. *Z. Phys.* **1959**, *155*, 206-222.

[2] Alder, J. F.; McCallum, J. J. *The Analyst* **1983**, *108*, 1169-1189.

[3] Numura, T.; Minemura, A. *Nippon Kagaku Kaishi* **1980**, 1621.

[4] Wessendorf, K. O. "The Lever Oscillator for Use in High Resistance Resonator Applications," *Proc. of the 1993 Frequency Control Symp.* (IEEE, New York, 1993).

[5] Schumacher, R. *Angew. Chem. Int. Ed. Engl.* **1990**, *29*, 329-343.

[6] Ward, M. D.; Buttry, D. A. *Science* **1990**, *249*, 1000-1007.

[7] Hillman, A. R.; Loveday, D. C.; Swann, M. J. *J. Chem. Soc. Faraday Trans.* **1991**, *87*, 2047-2053.

[8] Kanazawa, K. K.; Gordon II, J. G. *Anal. Chem.* **1985**, *57*, 1770-1771.

[9] Martin, S. J.; Granstaff, V. E.; Frye, G. C. *Anal. Chem.* **1991**, *63*, 2272-2281.

[10] Martin, S. J.; Frye, G. C.; Ricco, A. J.; Senturia, S. D. *Anal. Chem.* **1993** (In Press).

[11] Schumacher, R.; Borges, G.; Kanazawa K. K. *Surf. Sci.* **1985**, *L621*, 163.

Table I. Liquids shown in Fig. 10.

A	n-pentane	H	n-hexanol
B	n-hexane	I	n-heptanol
C	methanol	J	n-octanol
D	ethanol	K	dichloromethane
E	n-propanol	L	trichloroethylene
F	n-butanol	M	carbon tetrachloride
G	n-pentanol	N	dibromomethane

Figure Captions

Fig. 1. *Cross-sectional view of a smooth TSM resonator with the upper surface contacted by an ideal mass layer (at the interface) and a Newtonian liquid.*

Fig. 2. *Equivalent circuit model to describe the electrical characteristics (for f near f_s) of a TSM resonator under mass- and/or liquid-loading conditions.*

Fig. 3. *Resonator electrical admittance measured (points) and calculated (lines) near the fundamental resonance as the density-viscosity product ($\rho\eta$, g^2/cm^4-s) of a contacting fluid increases: (A) air, $\rho\eta = 2 \times 10^{-7}$; (B) water, $\rho\eta = 0.010$; (C) 43% glycerol in H_2O, $\rho\eta = 0.044$; (D) 64% glycerol in H_2O, $\rho\eta = 0.15$; (E) 80% glycerol in H_2O, $\rho\eta = 0.72$.*

Fig. 4. *Resonator electrical admittances measured (points) and calculated (lines) before and after deposition of a 124 nm Au layer. Before Au deposition: (A) in air, (B) in water; after Au deposition: (C) in air, (D) in water.*

Fig. 5. *Monolithic sensor that includes smooth and textured TSM resonators to measure liquid density and viscosity along with an RTD to measure temperature.*

Fig. 6. *SEM micrograph of surface corrugation, formed from electrodeposited gold, for trapping liquid at the surface.*

Fig. 7. *Schematic of instrumentation for operating dual-resonator sensor shown in Fig. 5 for liquid density and viscosity extraction.*

Fig. 8. *The difference in responses (Δf_1 - Δf_2) measured between the smooth and corrugated resonators upon immersion vs. liquid density. Liquids tested: (1) hexane, (2) butanol, (3) water, (4) chloroform, (5) carbon tetrachloride, (6) dibromomethane, and (7) tetrabromoethane.*

Fig. 9. *Changes in oscillation frequencies (upper) and motional resistances (lower) for smooth and corrugated resonators vs. the liquid parameter $(\rho\eta)^{1/2}$. The dashed line indicates network analyzer measurements.*

Fig. 10. *Scatter diagram comparing the extracted (circle) and literature (square) values of liquid density and viscosity for organic liquids listed in Table I.*

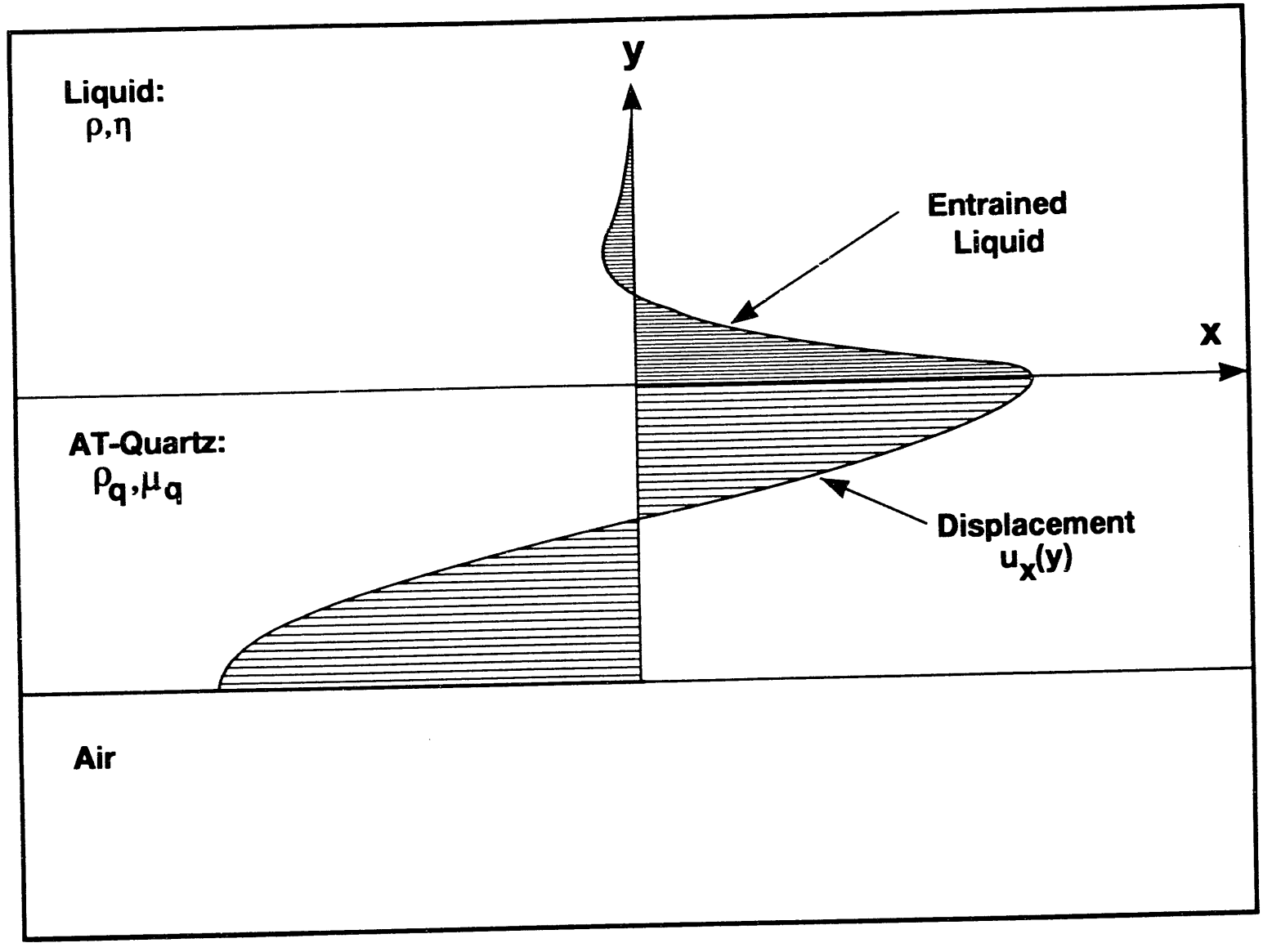

FIG. 1

T374A.AX3967.07

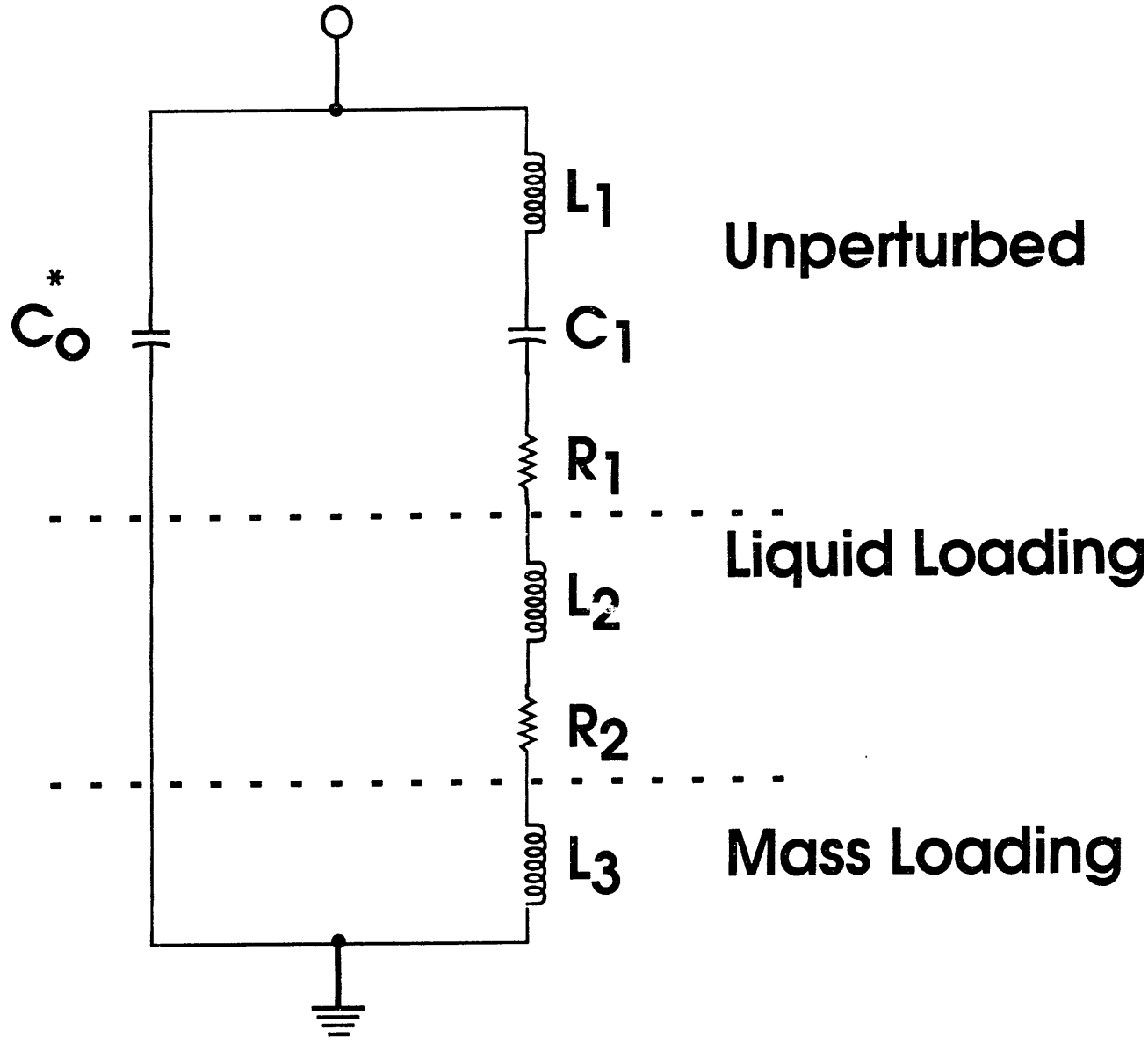

Fig. 2

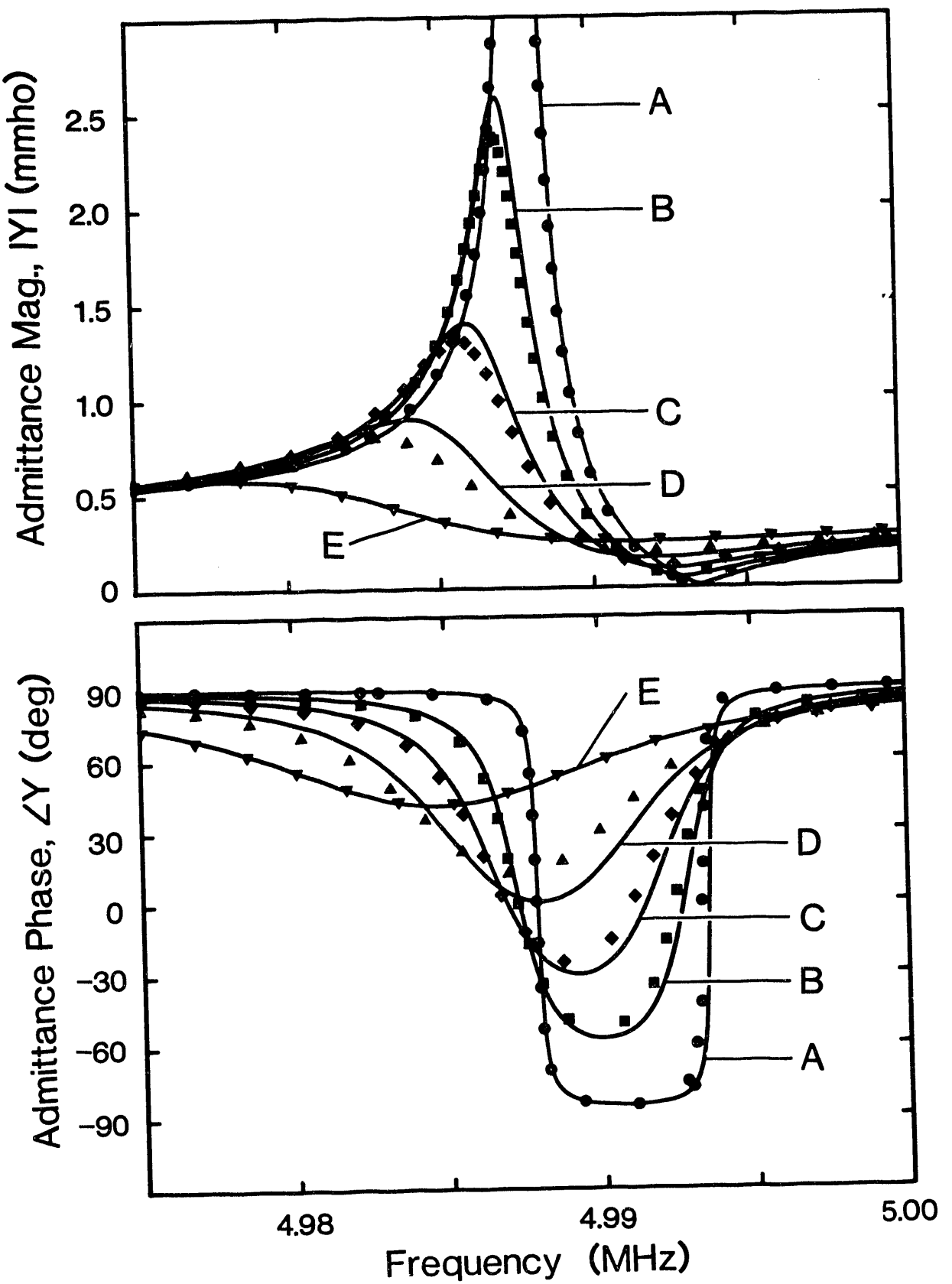
Admittance Mag., |Y| (mmho)
2.5
2.0
1.5
1.0
0.5
0
A
B
C
D
E
Admittance Phase, ∠Y (deg)
90
60
30
0
-30
-60
-90
E
D
C
B
A
4.98
4.99
5.00
Frequency (MHz)

Fig. 3

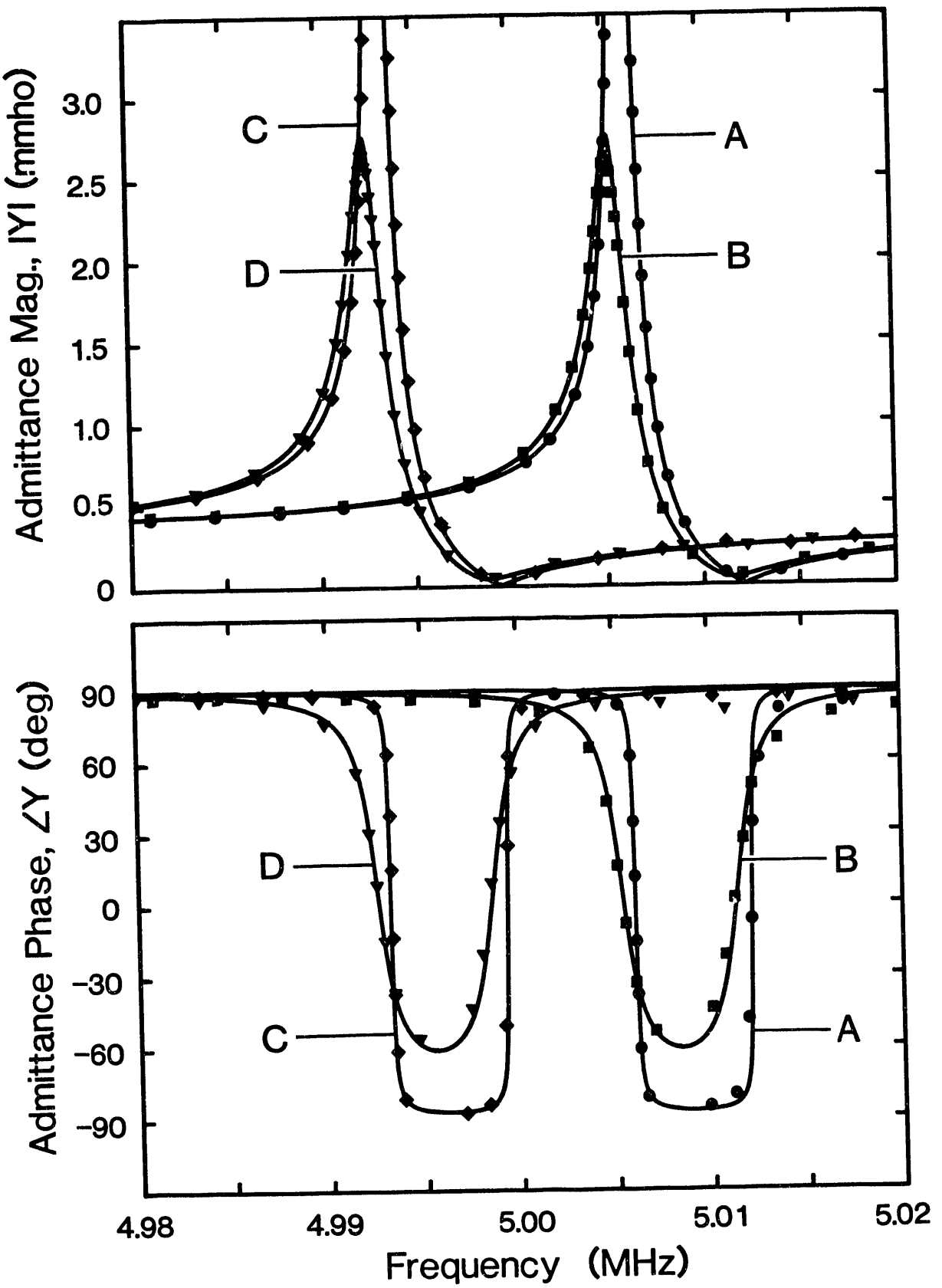
Admittance Mag., |Y| (mmho)
3.0
2.5
2.0
1.5
1.0
0.5
0
C
A
D
B
Admittance Phase, ∠Y (deg)
90
60
30
0
-30
-60
-90
D
B
C
A
4.98
4.99
5.00
5.01
5.02
Frequency (MHz)

Fig. 4

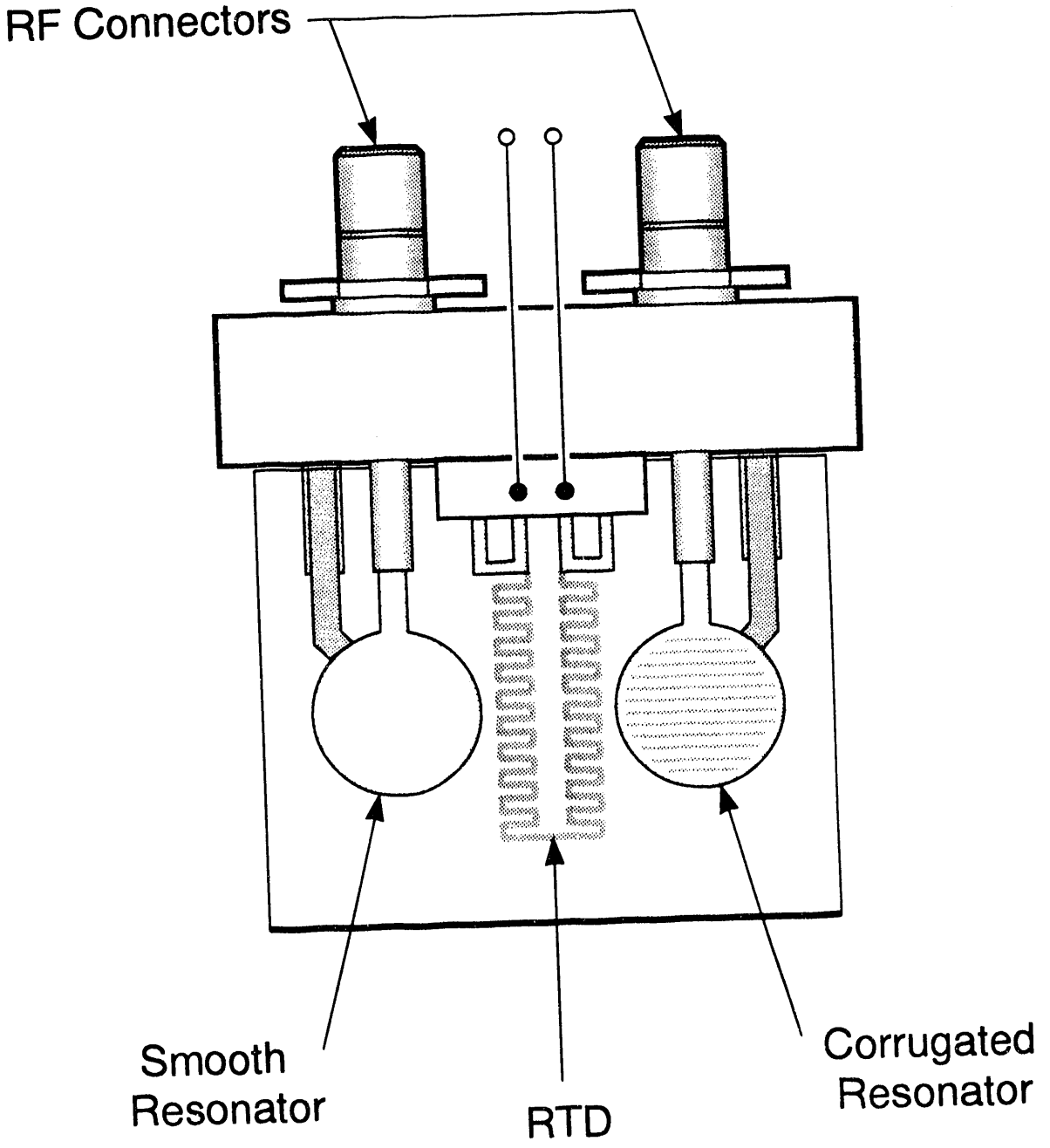

Fig. 5

T374A.AX3967.02

Untitled - 1

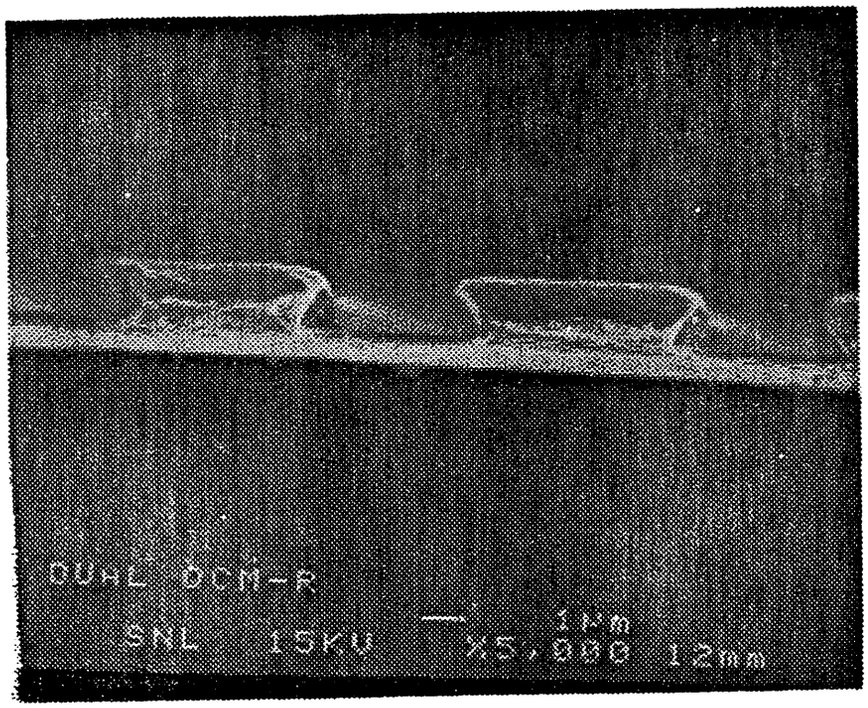

Fig. 6

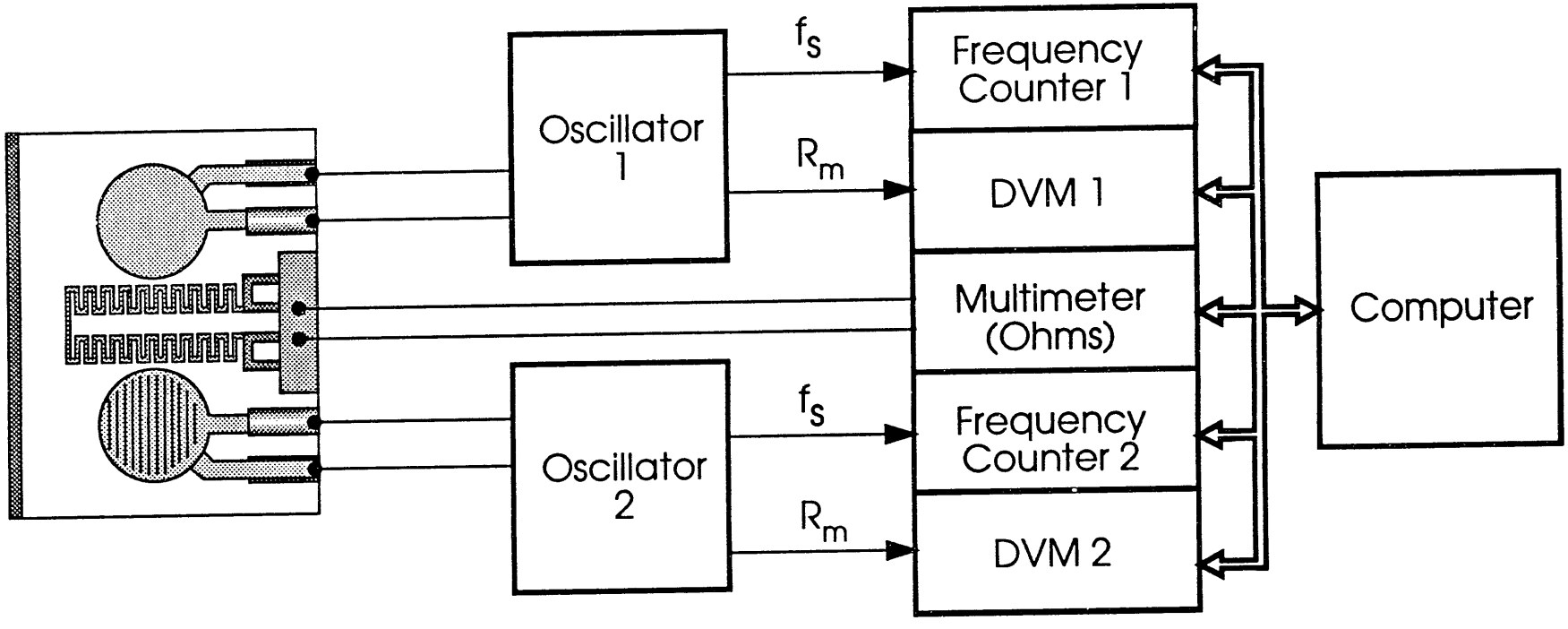
Oscillator 1
f_s
R_m
Frequency Counter 1
DVM 1
Multimeter (Ohms)
Oscillator 2
f_s
R_m
Frequency Counter 2
DVM 2
Computer

Fig. 7

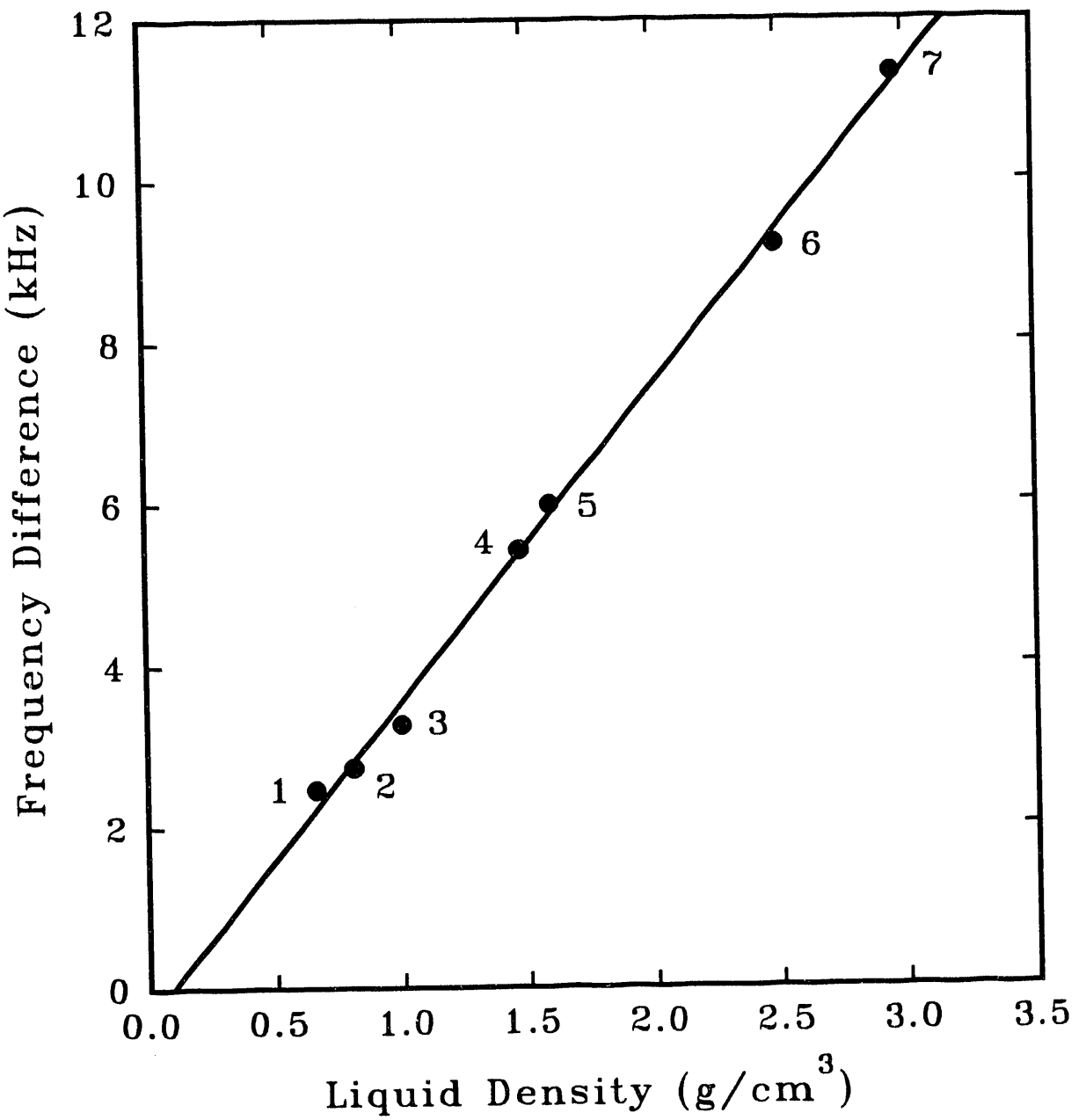

Fig. 8

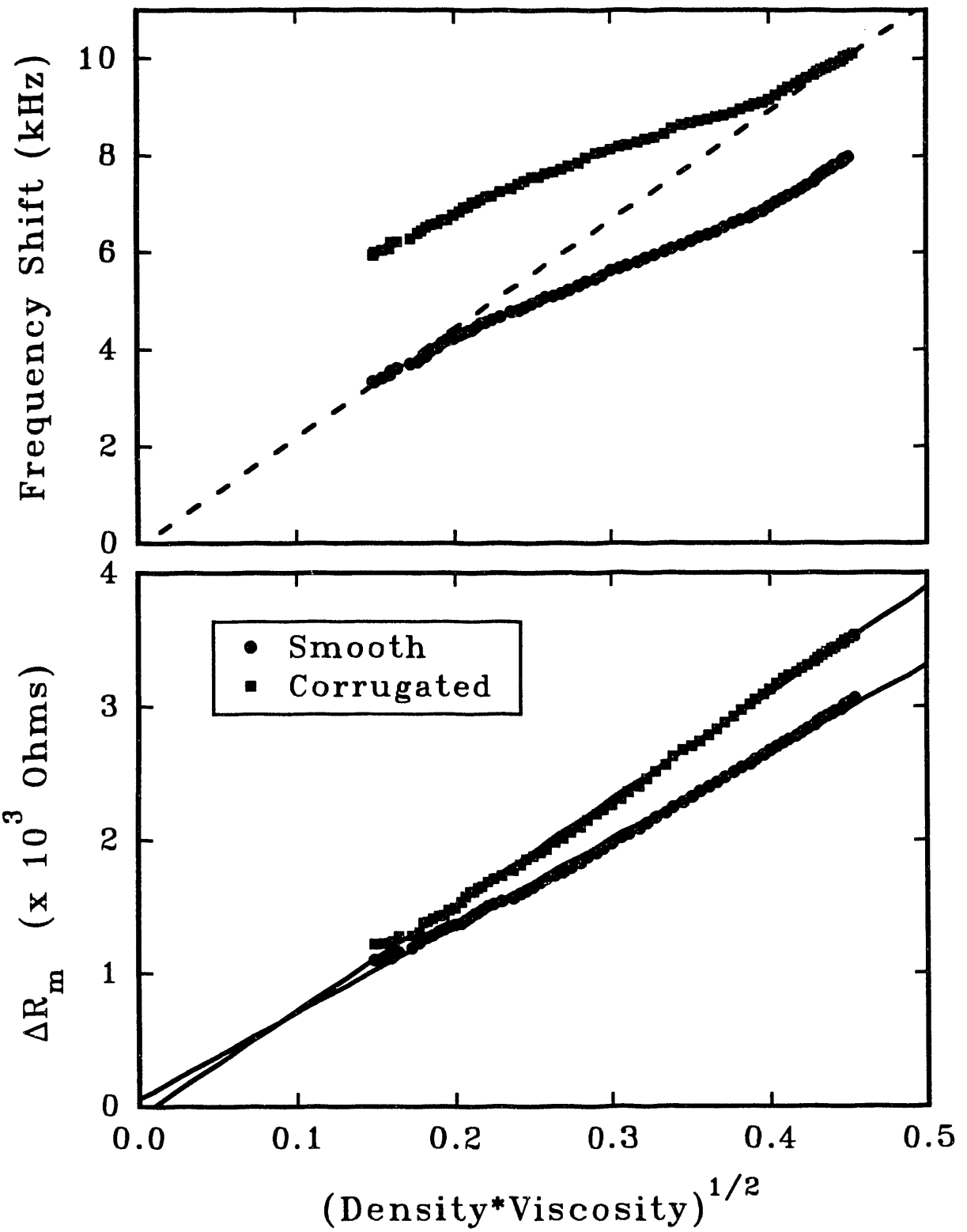

Fig. 9

file:DUAL4b.SP5

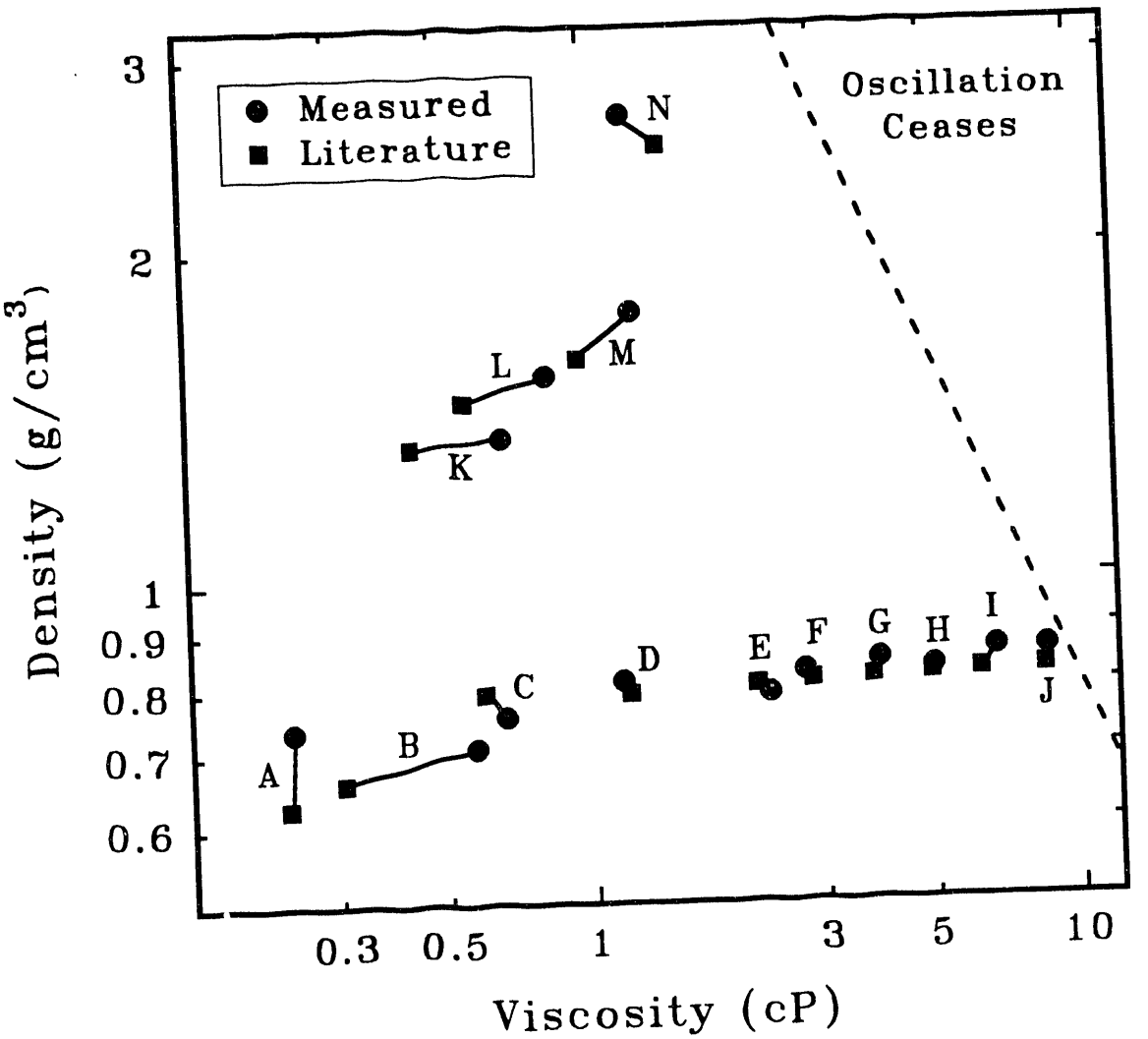

Fig. 10

file:LIQ52193.SP5 SJM

DATE
FILMED
10/27/93
END